Using plasma experiments to illustrate a complex index of refraction

W. Gekelman and P. Pribyl
Department of Physics and Astronomy, University of California, Los Angeles, California 90095

J. Wise and A. Lee
New Roads School, Santa Monica, California 90404

R. Hwang[a)]
Buckley School, 3900 Stansbury Ave., Sherman Oaks, California 91423

C. Eghtebas
University High School, Los Angeles, California 90025

J. Shin
Walnut Grove Secondary School, 8919 Walnut Grove Dr., Langly, Canada BC VIM2N7

B. Baker
University High School, Los Angeles, California 90025

(Received 13 July 2010; accepted 3 March 2011)

The index of refraction for the propagation of a wave in a plasma depends on the plasma density, background magnetic field, and frequency of the wave. The study of plasma wave propagation is an excellent tool for teaching students the subtleties involved in a complex media rather than in glass or water where the index of refraction is close to a constant. Whistler waves were launched and detected in a plasma physics laboratory at UCLA devoted to involving high school students and teachers. The magnetic field of the wave was measured in space and time and the wavenumbers at a variety of frequencies were determined. The index of refraction predicted by Appleton's equation was used to reconstruct the two-dimensional phase fronts and compared to the laboratory data with excellent agreement. The experimental techniques are discussed in conjunction with their use as an educational tool.
[DOI: 10.1119/1.3591341]

I. INTRODUCTION

Whistler waves[1] are electromagnetic waves that exist only in magnetized plasmas. Whistler waves near Earth are excited by high altitude lightning discharges.[2] The lightning discharge is an electric impulse that launches an electromagnetic wave, which travels to the Earth-ionosphere waveguide where it interacts with electrons to generate whistler waves. Whistlers are interesting because waves with different frequencies travel at speeds determined by the dispersion relation such that the field-aligned component at higher wave frequencies travels faster along the ambient magnetic field.

Whistler waves propagating in Earth's ionospheric plasma have frequencies low enough to be audible by the human ear. Whistlers were first noticed in 1886 on a 22 km telephone line[3] without amplification, but little was said or known about them. The first known report of a phenomenon resembling whistlers was published in 1894 by Preece,[4] the engineer-in-chief of a British telegraph company. The "whistles" were observed during a display of an aurora borealis at a British post office through telephone receivers connected to telegraphs. In 1919, another observation of whistlers was reported by Barkhausen,[5] who discussed conversations between soldiers in which they believed that gliding whistles heard during telephone communications were due to falling grenades. In 1925, the theoretical physicist and engineer Eckersley described disturbances that varied in duration and tone.[6] These disturbances were noticed when an audio recording system was connected to a large antenna. The noise began just above the highest audible frequencies and quickly decreased in pitch ending in a virtually constant low note. He attributed these disturbances to the dispersion of an electrical impulse.

The index of refraction of whistler waves is described for a cold plasma by the Appleton–Hartree[7] equation. The index of refraction depends on the local plasma density, the magnetic field, and the angle of wave propagation with respect to the magnetic field. Laboratory experiments that verify the wave propagation have been done in the linear[8] and non-linear regimes.[9] The complex index of refraction allows for the group and phase velocities of the wave to be different and explains the dispersion observed in the early observations. These waves are still of interest because of their importance in auroral physics of the Earth and other planets.

This paper is not an original study of whistler waves. Rather, it is an exploitation of the complex index of refraction to illustrate the intricacies of wave propagation. The waves were launched and detected in a small laboratory device dedicated to educational outreach at UCLA. We describe how the waves were launched and observed and used as an educational tool.

II. LAPTAG

The Los Angeles Physics Teachers Alliance Group (LAPTAG) Plasma Lab has met regularly at UCLA for the past 9 years. Over the years Laptag high school students have been involved in the construction of probes, amplifiers, antennae, machine shop fabrication, printed circuit etching and design, experimental design, and scientific programming for the analysis of data. LAPTAG is a voluntary effort of faculty and staff at UCLA, high school teachers, and high school students. Several junior college and college students have also attended. All students are welcome. There are no entrance or exit exams, certificates of completion, or course credit. The students involved are interested in science and are a

self-selected group. Incoming students find out about LAPTAG from their high school science teacher, the LAPTAG website,[10] or word of mouth.

III. EXPERIMENTAL SETUP

The LAPTAG plasma device used to conduct the whistler experiment was built by LAPTAG students and their faculty advisors. The device consists of a plasma source and a vacuum vessel in which the experiments are conducted, as shown in Fig. 1.

The plasma is created by an inductively coupled rf source[11] operating at up to 1 kW with Argon or Helium as the working gas. The source is pulsed with a repetition rate of 5–50 Hz with the plasma on time of $\tau_{on} = 4 - 10$ ms, and operating at a radio frequency (rf) of 400 kHz. The field coils surrounding the chamber make an axial magnetic field ($20 < B_{0z} < 120$ G). (B_{0z} is the constant background magnetic field in the z direction.) The experiments have a very repeatable afterglow period, that is, the time after the rf source is switched off. This pulsed source enables experiments to be performed in this quiescent plasma ($\delta n/n, \delta T/T < 1\%$). The plasma density is $10^8 \leq n \leq 10^{12}$ cm^{-3}, and the electron temperature T is 3 eV during the rf discharge and rapidly decays to 0.4 eV in the afterglow. The argon ions are cold, with energies less than 0.2 eV. Under typical conditions, the electron gyroradius is 0.2 mm, the ion gyroradius is 5 cm, and the Debye length is 15 μm.

The whistler experiment takes place on a microsecond time scale, typically 0.1–1 ms after the start of the plasma afterglow period. The density is approximately constant during the whistler measurements, which last less than one half a microsecond. The timing of the experiment is shown in Fig. 2. In this case, the experiment is repeated at 10 Hz, which allows for efficient signal averaging at each position at which the data are acquired. The timing is highly reproducible, and the time in the afterglow during which the experiment is carried out as well as the wave tone burst, that is, a phase locked burst of a fixed number of cycles, is the same from shot to shot.

The whistler wave is produced using a single turn magnetic loop as a launcher. The experimental setup is shown schematically in Fig. 3. A narrow pulse ($V_{pp} = 0.5$ V,

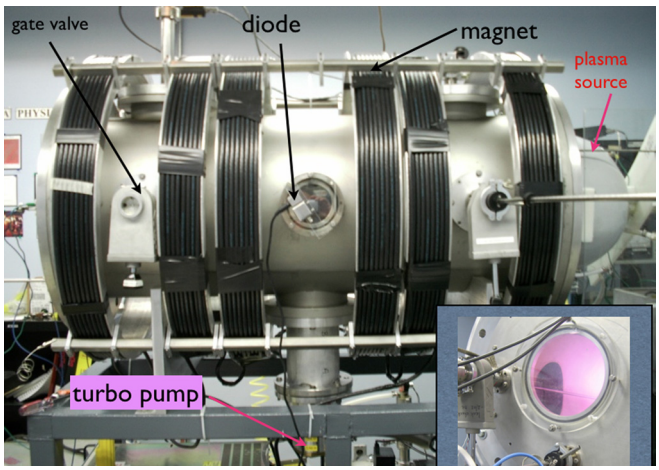

Fig. 1. LAPTAG experimental device. The cylindrical chamber is 1.5 m long and 0.4 m in diameter. The chamber vacuum ($2–3 \times 10^{-6}$ Torr) is attained using roughing/turbo pumps and then filled using a mass flow controller (MFC) to a working pressure of 1 to 25 mTorr of argon. The axial solenoidal magnetic field is produced by the coils. An inset showing the glowing plasma is on the bottom right.

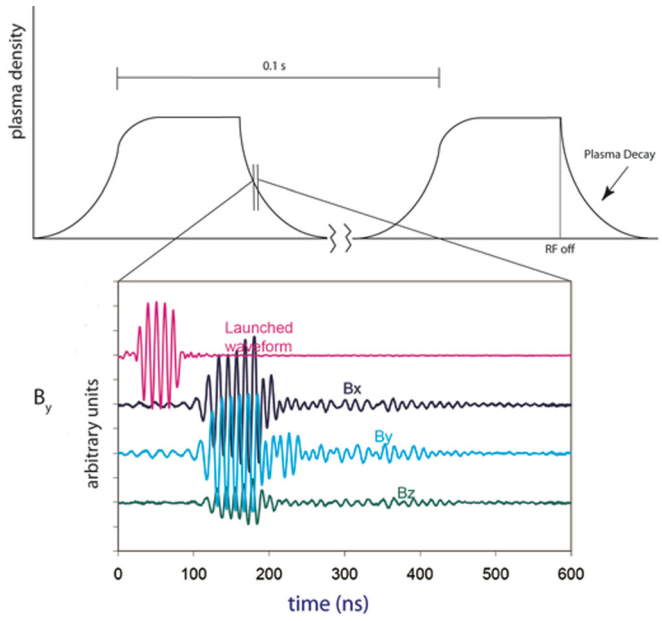

Fig. 2. Timing diagram for the experiment. The rf source is pulsed on for 5 ms at 10 Hz, and the whistler waves are launched and detected in the plasma afterglow while the density is still substantial, the plasma is extremely quiescent, and there is no signal noise introduced by the rf source.

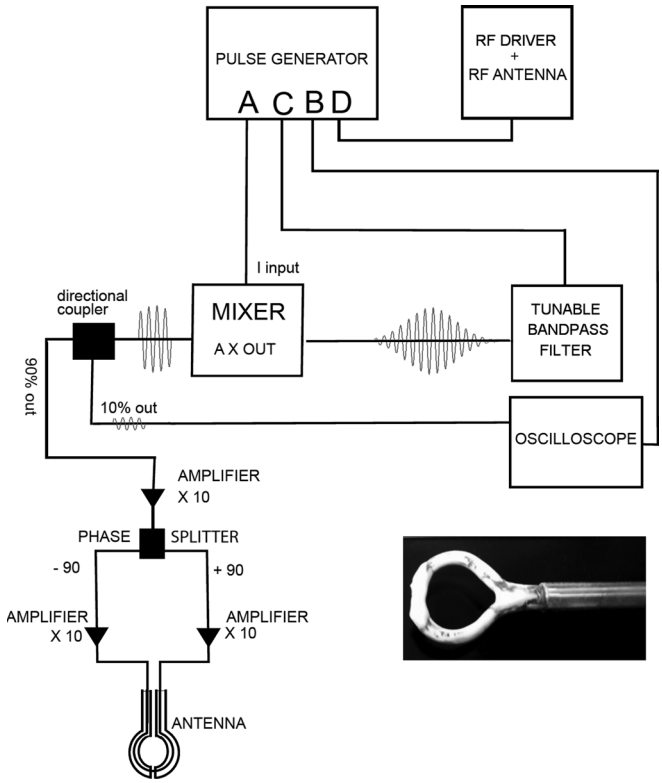

Fig. 3. Schematic diagram of the experimental setup. The whistler wave antenna is driven symmetrically at $60 < f < 120$ MHz with approximately 0.5 W. A pulse generator with four outputs, *A*–*D*, sequences the experiment. A 20 μs pulse from output *C* forms the input into a tuned resonator (here shown set to 60 MHz), the leading edge of which results in a wave train at the resonant frequency. The mixer, using a pulse from channel A on the I input, acts as a switch to select a few cycles from this wave train to generate a tone burst of a few cycles. Three to five cycles from the center of the tone burst are selected and then amplified and sent to the phase splitter where the input signal is divided into two output signals shifted 180° out of phase; these are amplified again to symmetrically drive the antenna. A photograph of the antenna is inserted on the bottom right. The antenna diameter is 1.3 cm.

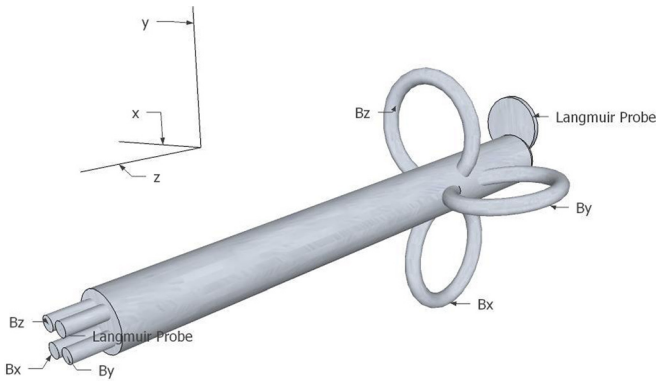

Fig. 4. Schematic diagram of the three-axis magnetic probe and Langmuir probe. The z-axis corresponds to the machine axis and is the same as the direction of the background magnetic field. The outer diameter of the magnetic B-dot probes is 7 mm. The Langmuir probe is a copper disk with a diameter of 5.3 mm.

$\delta t = 0.1$ μs, where the subscript "pp" means peak to peak and δt is the pulse length in microseconds, is fed to a narrow band tunable filter (tuned to 60 MHz). The filter output is sinusoidal and rings for approximately 20–40 periods at the resonant frequency. The filter output is sent through a mixer that acts as a switch to extract a short tone burst $\delta t_{\text{burst}} = 5$ periods. The tone burst is amplified and symmetrically fed into a single turn magnetic loop consisting of a coaxial wire with a solid outer shield, bent into a loop of 1.5 cm diameter, as diagrammed in Fig. 3. Two signals 180° out of phase are applied to the coaxial center conductors, outside the vacuum system. In the center of the loop, a section of the shield of the coaxial cable is removed to make a small gap (<2 mm), allowing the changing magnetic flux in the cable to escape.

The changing magnetic field produced by the antenna is at right angles to the background magnetic field, and the resulting plasma response is a whistler wave. The whistler wave has three spatially and temporally varying magnetic field components (as well as three electric field components), even though the launching antenna couples primarily to only one of them ($B_{y\text{-wave}}$). The launcher behaves approximately as a point source for the wave because its diameter is a small fraction of the parallel wavelength.

The whistler detector (see Fig. 4) is a three-axis magnetic pickup probe. Each axis has a single loop of coaxial wire with a gap (as in the exciter antenna) to allow sensitivity to a changing magnetic field within the loop. By Faraday's law, the electric field at the end of the loop is $E = -d\phi/dt$, $\phi = BA$, where ϕ is the magnetic flux threading the loop and A is the area of the loop (see Fig. 5). The probe is mounted on a stainless steel shaft, which passes through a double O-ring seal to allow motion along B_{0z} as well as transverse rotation while maintaining vacuum. A Langmuir probe is also mounted in close proximity to the three magnetic pickups.

IV. DATA COLLECTION

The probe shaft goes through a sliding seal located on the end of the chamber opposite to the plasma source. The shaft penetrates the chamber well off-center from the plasma, and the probe assembly is mounted on an L-shaped ceramic holder so that the probes pass through the center of the plasma. There are two stepping motors that move the probe shaft. The first is in the axial (z) direction, which is parallel to the magnetic field, and the second rotates it about z. The rotation sweeps the B-dot/Langmuir probes across an arc that approximates a transverse section of the plasma. The data are collected over two spatial dimensions using the computer controlled probe drive. A 2.5 Gs/s (bandwidth equal to 440 MHz) digital oscilloscope is used to acquire the data at each spatial location. A LABVIEW™ program controls the probe drive and the digital oscilloscope.

Three components of the wave's magnetic field and the plasma density are collected at each position. The data are collected in 1 cm intervals along the z-axis, and the x-axis position is determined by taking the sine of the angle that the probe is rotated, and multiplying it by the length of the arm from the shaft of the probe. For this series of runs, data are collected over an axial distance of 60 cm and a transverse (x) position varying over −8.6 to 8.6 cm from the center.

V. THEORY OF WHISTLER WAVE DISPERSION

The index of refraction μ is the ratio of the speed of light to the speed of the propagating whistler wave, $\mu = kc/\omega$. For light in vacuum, or a simple medium such as glass, the index of refraction is a constant independent of the direction of propagation. In contrast, the index of refraction for waves in plasmas is usually complicated, and that for whistler waves is no exception. For whistler waves, μ depends on the plasma density n (or the equivalently electron plasma frequency f_{pe}), the background magnetic field B (or equivalently the electron cyclotron

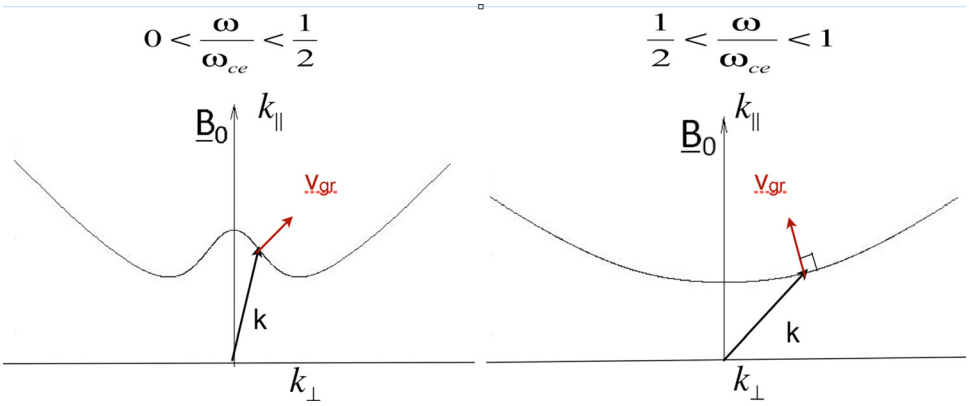

Fig. 5. Wavenumbers at a fixed density for cases where the wave frequency is above or below half the electron cyclotron frequency. Note that the group velocity is perpendicular to the line at the point of intersection with $\vec{\mathbf{k}}$.

frequency f_{ce}), the whistler wave frequency f, and the angle θ of the wave propagation with respect to the background magnetic field. The wave is also damped by collisions between electrons and neutral gas atoms, which can be modeled by a simple collision frequency ν_{en}. The index of refraction μ in terms of these parameters is given by Appleton's equation[12]

$$\mu^2 = 1 - \frac{X}{1 - iZ - \frac{0.5Y_T^2}{1 - X - iZ} \pm \frac{1}{1 - X - iZ}\left[\frac{1}{4}Y_T^4 + Y_L^2(1 - X - iZ)^2\right]^{\frac{1}{2}}}, \tag{1}$$

where $X \equiv f_{pe}^2/f^2$, $Y \equiv f_{ce}/f$, $Y_T = Y\sin\theta$, $Y_L = Y\cos\theta$, θ is the angle between $\vec{k}$ and $\vec{B}_{0z}$, where $\vec{\mathbf{k}}$ is the wavenumber, $|\vec{\mathbf{k}}| = k \equiv 2\pi/\lambda$, and the direction of $\hat{\mathbf{k}} = \vec{\mathbf{k}}/k$ is along the propagation of the wave phase fronts, and $Z \equiv \nu_{en}/2\pi f$. In our case $f_{pe} = \sqrt{ne^2/m_e\varepsilon_0} \approx 8.98 \times 10^3\sqrt{n}$, where the plasma density n is given in cm^{-3}, $f_{ce} = 2.8 \times 10^6 B(\text{Gauss})$, and Z is the ratio of the electron neutral collision frequency, which causes damping of the drive frequency to f_{wave} of the wave. The angle between the wave propagation direction, parallel to $\vec{k}$ and the magnetic field, is θ. In this experiment, typical frequencies were $32\ \text{MHz} \le f_{wave} \le 90\,\text{MHz}$, $2.0\,\text{GHz} \le f_{pe} \le 7.2\,\text{GHz}$, $112\ \text{MHz} \le f_{ce} \le 280\,\text{MHz}$, and $0.001 \le \nu_{en}/\omega_{wave} \le 0.01$.

Appleton's equation is based on several assumptions: The ions are cold and form a motionless background. This assumption is a good approximation in our experiment because the ions move only about 1 mm during the time of 500 ns. The electrons are cold, which is also a good assumption because at the time the experiment is performed the electron temperature is about 0.5 eV or less. It is also assumed that the waves are linear and the solution to the wave equation can be Fourier analyzed. (The more advanced students in the group have learned what each of these assumptions means.)

In this study, we used whistler waves to learn about the index of refraction. For example, the whistler phase and group velocities, unlike those of light, can be different. The phase velocity is that of a crest moving within a whistler wave packet of several cycles. The group velocity is that of the wave packet itself. These velocities are defined as

$$\vec{v}_{phase} = \frac{\omega}{k}\hat{\mathbf{k}} \quad \text{and} \quad \vec{v}_{group} = \frac{\partial\omega}{\partial\vec{\mathbf{k}}}, \tag{2}$$

The phase and group velocities differ in both magnitude and direction for a given frequency. This difference makes the study of the index of refraction for whistlers highly motivating to students and gives them opportunities to apply higher levels of mathematics, data analysis, and reporting. Figure 5 illustrates the relation between the group and phase velocity.

The line in Fig. 5 is the solution to Eq. (1) for a given field, density, and ω, for the case in which there are no collisions ($Z = 0$). For a fixed frequency, a large range of wavenumbers is possible. The wave does not exist above the electron cyclotron frequency. The k vector is a line from the origin to a point on the curve $(k_\perp, k_\parallel)$. The group velocity vector is perpendicular to the tangent to the curve at the point of intersection with $\vec{k}$. If a single frequency wave is launched from a point source, the spatial pattern of the wave is a superposition of waves with all allowable $\vec{k}$ vectors.

The predicted behavior of the index of refraction as a function of propagation angle for typical LAPTAG plasma parameters is shown in Fig. 6. Consider the index of refraction for a wave at 30 MHz [see Fig. 6(a)]. It becomes large for angles $\theta > 40°$, and therefore the wave does not propagate because $k = 2\pi/\lambda \to \infty$ implies that the wavelength goes to 0. For waves in a plasma, if the wavelength approaches the electron cyclotron radius, the wave becomes heavily damped. At a given frequency, density, and magnetic field, the whistlers propagate at all angles inside a cone,[13] the axis of which is aligned along the magnetic field. Figure 7 is a plot of the wavenumbers (see Fig. 5) for the experimental conditions described in Sec. VI.

VI. EXPERIMENTAL RESULTS

The data are best understood in stages. We present in Fig. 8 the wave propagation along the background magnetic field. The antenna is placed in the center of the plasma,

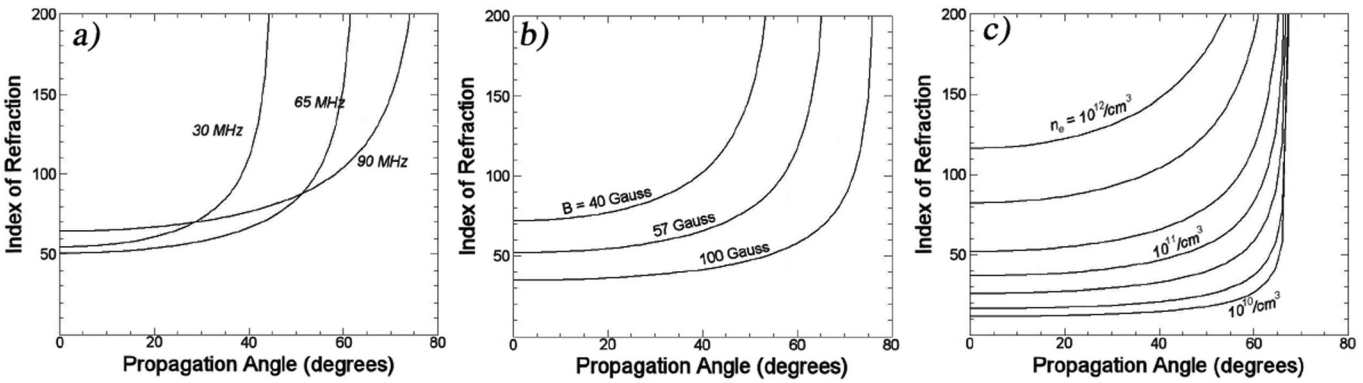

Fig. 6. The index of refraction calculated from Eq. (1) for densities, magnetic fields, and frequencies typical of the LAPTAG experimental conditions. (a) $n = 2.0 \times 10^{11}\ \text{cm}^{-3}$, $B = 57$ G; (b) $n = 2.0 \times 10^{11}\text{cm}^{-3}$, $f_{wave} = 60$ MHz; (c) $B = 57$ G, $f_{wave} = 60$ MHz.

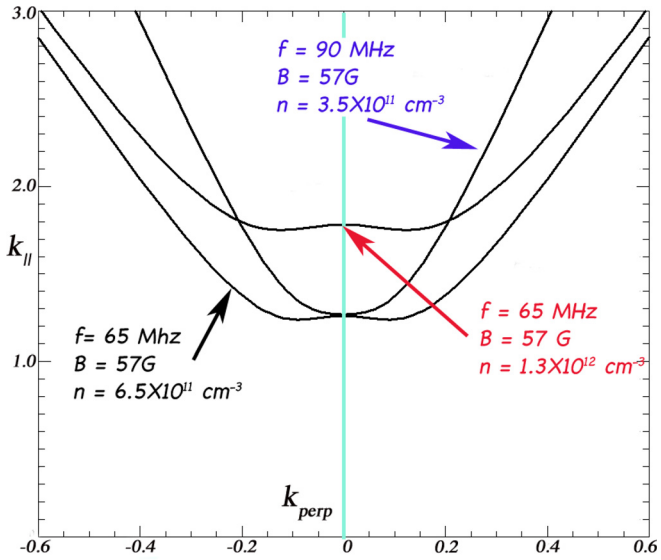

Fig. 7. Parallel and perpendicular wavenumbers for the three cases analyzed in detail. Note that a B vector at a given angle is a vector drawn from the origin to a point $(k_\perp, k_\parallel)$ on one of the curves. The $\boldsymbol{k}$ vector points in the wave phase velocity direction.

$x = y = z = 0$ (for all cases), and the three-axis magnetic field probe is moved along the direction of the background, constant magnetic field $\vec{\mathbf{B}} = B_{0z}$. Time is defined with respect to the launch of the whistler wave burst. In Fig. 8, one component of the magnetic field is shown, $B_y(z,\ t = 280$ ns), and therefore the distance between crests of the wave is the wavelength $\lambda_p = 12$ cm.

The wavefronts of one component of the field can be plotted at a fixed time and in space as a surface plot. Figure 9 shows $B_y(x, z)$ at three times. As in the space-time diagram of Fig. 8, the wave crests can be followed to determine the wave phase velocity. The data in Fig. 9 were acquired for a different frequency tone burst and different background field from that in Fig. 8, and therefore the phase velocity is different. The three orthogonal magnetic probes record a signal proportional to $d\vec{\mathbf{B}}/dt$, and because the wave is at a fixed frequency, the probe signals are also proportional to $\omega\vec{\mathbf{B}}$. The time history of all three components of the field is known at every spatial location on the data plane and the full vector field can

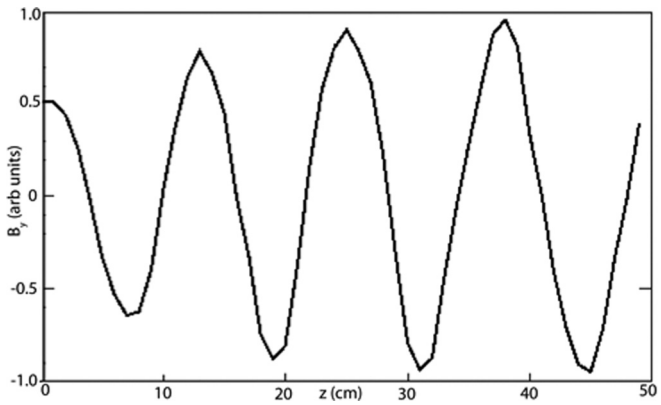

Fig. 8. Propagation of one component, B_y, of the whistler wave along the background magnetic field. $T = 280$ ns from the start of tone burst, $f = 65$ MHz. The wavelength may be read from the graph as $\lambda = 12$ cm, $k = 0.53$ cm^{-1}. Data are acquired for all three components, $\vec{B}(z, t)$ at each of 61 axial locations and 1250 time steps.

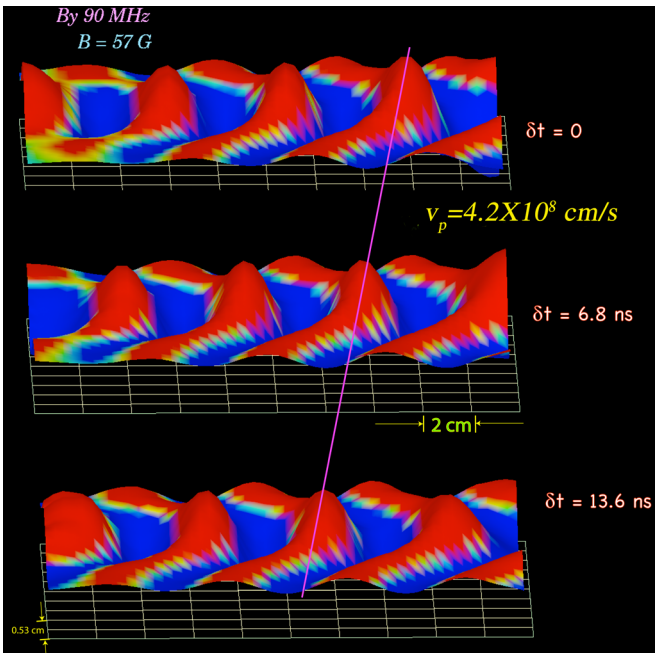

Fig. 9. 90 MHz tone burst with $f/f_{ce} = 0.56$, $f/f_{pe} = 0.017$. The launch antenna is located at $z = 0$. B_y is given in arbitrary units. By following a wave crest as a function of time, the phase velocity of the wave can be measured.

be displayed as in Fig. 10. The vector field is shown at two times one half cycle apart. When viewed as a function of time, the vectors at the rear rotate counterclockwise, the same direction as the electron gyro motion. Whistlers are electron waves. The full three-dimensional motion, which is better appreciated in a movie (online animation of Fig. 10 with $\Delta t = 0.40$ ns), reveals more complicated rotation with components about the x and y axes as well.

VII. COMPARISON OF EXPERIMENT TO THEORY

An excellent way to insure that the waves are whistlers is to measure the dispersion relation, the dependence of propagation speed on frequency. This measurement is an integral part of the educational component of this lab activity. The wave frequency was varied (at a constant plasma density and magnetic field) and a series of plots similar to Fig. 8 were generated. The wavenumber on a line along the background field passing through the center of the antenna ($\theta = 0$) was measured, and the resulting dispersion is plotted in Fig. 11. There are no data at small parallel wavenumbers because the wavelength approaches or exceeds the machine length. Waves with large wavenumbers ($k_\parallel > 0.6\,\text{cm}^{-1}$) are heavily damped.

We next examined three cases of whistler wave propagation. The wave fronts, such as those in Fig. 9, are due to a superposition of waves with different k vectors at a fixed launch frequency. The parallel and perpendicular wavenumbers for the three cases are shown in Fig. 7. To compare the measurement to theory, we assume that the antenna is a point source for whistler waves (the antenna is much smaller than a parallel wavelength). For fixed ω, we find all the possible $\mathbf{k}$ vectors from Appleton's equation. We then draw the superposition of plane waves having the appropriate $|\mathbf{k}|$ and traveling at the correct angle θ with respect to the magnetic field. For light, the dispersion relation is $\omega/k = c$, and the propagation is isotropic in vacuum. Figure 12 illustrates the process of summing light waves propagating at all angles, showing the

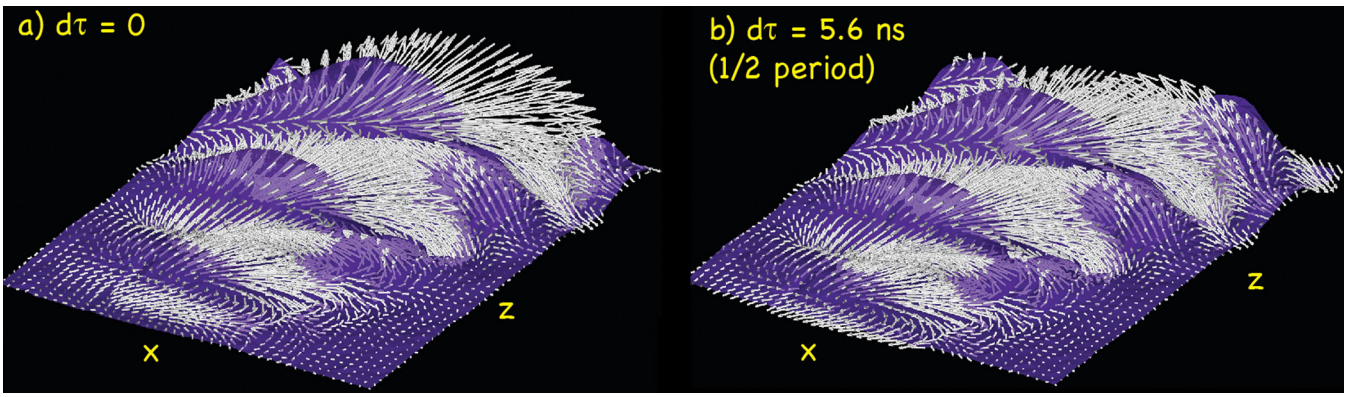

Fig. 10. Diagram of the measured vector magnetic field in the x–z plane at two times which are $\frac{1}{2}$ period apart; $f = 90$ MHz. The arrows on the far side (closest to the antenna) rotate in a counterclockwise direction about B_{0z}. The total rotation is three-dimensional, which can be seen in the accompanying movie (enhanced online) (Ref. 21). [URL: http://dx.doi.org/10.1119/1.3591341.1]

result of adding progressively more waves to the picture. The addition of 100 waves with the same phase velocity but at different propagation angles approximates a spherical wave.

The index of refraction for whistler waves μ depends on the angle for fixed ω, B, and n, as given in Eq. (1). This dependence means that when we compute the sum to generate a simulation of the whistler waves (analogous to Fig. 12), the wavenumber at every propagation angle is different, and the waves do not sum to give a sphere. An equivalent statement is that the waves' velocities depend on their angles of propagation. The sum for the three sets of experimental conditions that were studied is compared to the measurement in Fig. 13. One hundred plane waves, each having its angle-dependent wavenumber computed by Eq. (1), were superposed. The experiment and the computation matched well despite the assumptions we made.

In the simulation, the plasma density and background magnetic field were constant over the plane. Langmuir probe measurements, as well as measurement of the background magnetic field with a Hall probe, showed this assumption to be reasonable. The measurement of the electron temperature by a Langmuir probe at the time that the wave was launched, $T_e < 0.5$ eV, justified the assumption of a cold plasma in Eq. (1).

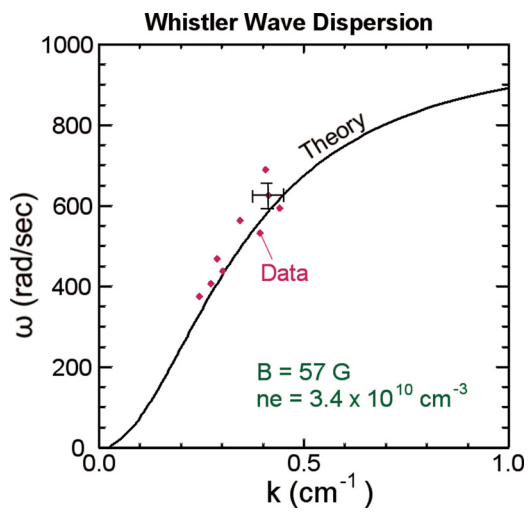

Fig. 11. Theoretical dispersion relation and experimental data for parallel propagation. The uncertainty in ω comes from the finite length of the tone burst, $\Delta f \Delta T \approx 1$.

VIII. WHISTLER WAVE EXPERIMENTS AND LEARNING THE PROCESS OF SCIENCE

LAPTAG is a unique opportunity for students to participate in STEM (Science, Technology, Engineering, and Math) education and the process of science. By using plasma physics as an educational "hook," students are engaged in a series of experiments, lectures, presentations, and group discussions. Learning happens during initial discussions, topics are "relearned" as the experiments are done, and probably the greatest and most exciting learning occurs in planning for presentations. The students have presented their results at AAPT (Ref. 14) and APS (Ref. 15) meetings and participated in a Physics Department Colloquium at Cal-State Los Angeles. Because the students are the actual presenters, they develop a much deeper understanding of the concepts.

Students experience the process of science first hand. Students are involved in the planning of all experiments. We first discuss the limitations of our machine, the need for any necessary purchases or fabrications. What type of antenna is necessary to launch the wave and how does it work? Amplifiers for the antenna and the receiver have to be constructed. The students learned the elements of their operation (they would not be able to design them) and soldered the components together. The B-dot probe was designed and entirely constructed by the students. Experimental results need to be extracted from noise. Students learned about data filtering and smoothing as they looked at the data for meaning. The data analysis programs were written by students. Learning from matching theory with experimental results gave students experience in the practice of science.

The outcome is that students are better prepared to enter the STEM pipeline by gaining a deeper understanding of the scientific method, and in this case, the concept of the index of refraction and its effects on wave propagation. For example, students comprehend such advanced topics as dispersion, k-space, plasma properties, and wave group and phase velocities. This engagement supports efforts to improve STEM career choices by exposing high school students to challenging and interesting experiences in preparation for advanced study.

Bloom[16] identified a three state model for talent development. First, a teacher helps a student develop a love for mathematics and/or science. Another teacher provides instruction on the rules, content, and skills that allows

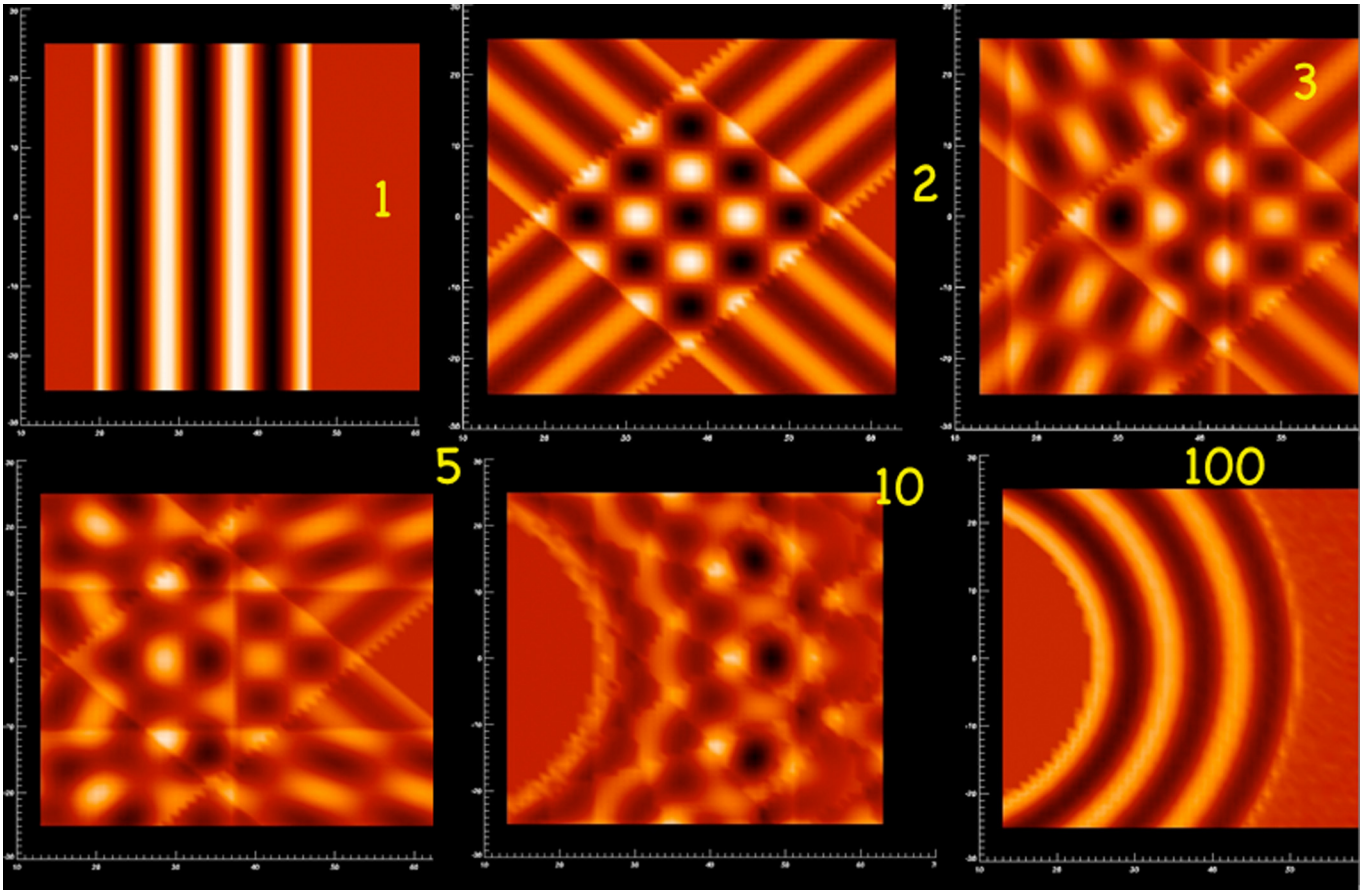

Fig. 12. Wave summation for isotropic wave propagation, such as for light in a vacuum. The sequence of figures illustrates the process of summing up progressively more plane waves propagating outward from a source at the left, with the result being circular phase fronts. The figures are labeled by the number of waves that are summed. For one wave, a single plane wave $\theta = 0$ comes from the virtual source at the left, and propagates to the right; Two plane waves propagating at $\theta = \pm 45°$, three waves (equivalent to the sum of one and two waves); five waves (equivalent to the sum of three waves and $\theta = \pm 90°$); the 10 and 100 wave summations are at equispaced angles. The summation of 100 plane waves results in an approximately circular wavefront propagating outward in all directions from a virtual source.

students to access the field. At this point, students begin to identify themselves as novice scientists or mathematicians. Lastly, students are presented insider knowledge associated with a given field. This process is the LAPTAG model.

Brody[17] has provided expected short-term assessment outcomes for programs designed to improve the STEM career pipeline. He suggests evaluating the following:

- Learning of content: At some level, knowledge of scientific principles, enhancement of technical or problem solving skills, or other preparation for more advanced work should be expected. Clear evidence for such learning is provided by the students' participation in poster and paper submissions.[14,15,18] These efforts develop and display improved knowledge and preparation for more advanced work.
- Enhanced positive attitudes—even excitement—toward the discipline: Positive attitudes toward STEM fields, and physics in particular, are evidenced by student participation over the years. Some students have been in LAPTAG for three years or more.
- Increased self-confidence in one's ability to excel in this field: We often see students' self-confidence improve as they master complex concepts and data analysis techniques. Students, who have been very shy at first, have demonstrated pride and confidence in later presentations.
- Increased knowledge of the value of mathematics and science in the workplace and increased awareness of mathematics and science careers.
- Removal of any barriers to possible advancement in mathematics and science that existed prior to the intervention.

Some students come from public schools where access to higher mathematics and science programs is limited. Even students coming from schools that do provide advanced classes find themselves challenged beyond the existing curriculum because as a working research lab, LAPTAG takes them out of the artificialness of science in the classroom and gives them the opportunity of doing science.

Success in STEM fields requires a commitment of time and effort. What causes LAPTAG students to commit their time and effort? Although a portion of a student's commitment to STEM studies comes from how well a student performs, there is also a component of commitment developed by how well students are able to match their image of the discipline with their own perceived self-image. Hannover and Kessels[19] provide evidence that students rate science-interested students lower than others in physical and social attractiveness, social competence, and integration. Science-interested students are also rated higher in intelligence, motivation, arrogance, and self-centeredness. It is clear that the prototype of students who like science is less favorably

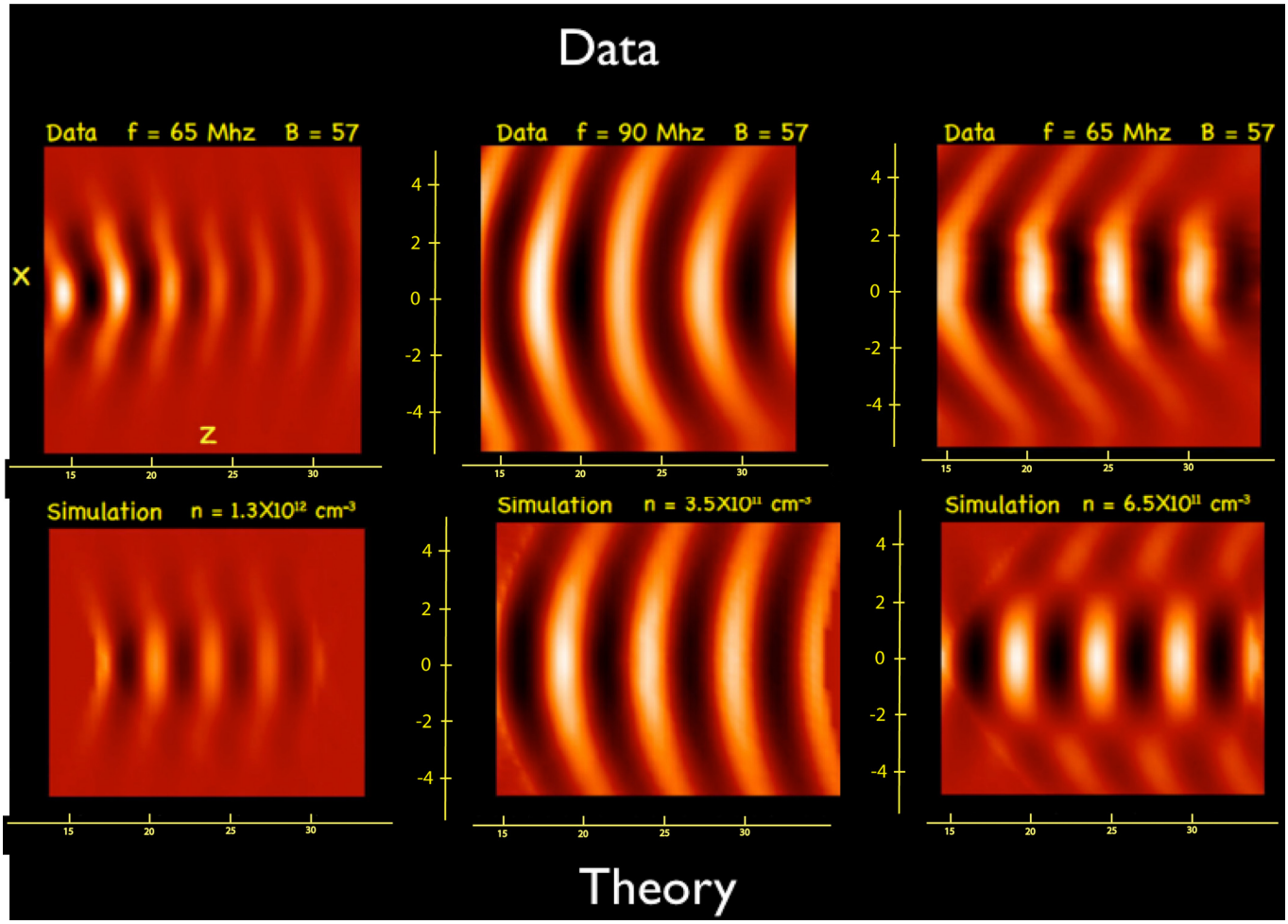

Fig. 13. Measured data (top row) and theoretical comparison (bottom row) of B_y for whistler waves for the three experimental conditions described in the text. In all cases, the structures shown in the screenshots propagate to the right with no significant modification of their shapes. The pictures were computed by superposing 200 plane waves, each propagating at a different angle and each with the appropriate phase velocity computed from Eq. (1). The scales in z (abscissa) and x (ordinate) are different, and the distances are in centimeters.

viewed by peers than those who do not like science. LAPTAG shatters many myths about science as a discipline and scientists as people.

LAPTAG also prepares students for STEM disciplines by introducing professional norms to prepare students for the standards of professional practice.[20] This preparation gives the students the confidence and competency to fully participate in undergraduate classes and the vision of the "end game" to keep them motivated to persevere in difficult times.

LAPTAG's students are at all levels of intellectual development. Some have mastered the concepts, while recent members have a more superficial understanding. By using this study of the index of refraction, students at all levels learned, or were exposed to, the process of science, experimental design, the properties of waves, applications of mathematics, and instrumentation and computers.

IX. SUMMARY

The plasma lab has provided content knowledge and understanding of the index of refraction and the process of science using whistler waves. Other experiments are planned, but in all our efforts, students are exposed to strong content knowledge in mathematics and science based on academic instruction and hands-on demonstration, appreciation for the utility of STEM subjects in the workplace, role models working in STEM fields, and peers who share interests in STEM areas of study.

ACKNOWLEDGMENTS

The authors would like to thank Z. Lucky, M. Drandell, and M. Nakamoto (all at UCLA) for their technical assistance. They also acknowledge the help of A. Levy (Santa Monica Community College), A. Martinez (New Roads School), and E. Hobel (Buckley School). This work was done at the Basic Plasma Science Facility at the University of California, Los Angeles. The Basic Plasma Science Facility is funded by the Office of Fusion Science at the Department of Energy and the National Science Foundation.

[a]Present address: Princeton University, Princeton, New Jersey 08544.

[1]R. Helliwell, *Whistlers and Related Ionospheric Phenomena* (Stanford University, Stanford, CA, 1965).
[2]D. D. Sentman, "Preliminary results from the Sprites 94 aircraft campaign," Geophys. Res. Lett. **22**, 1209–1212, (1995).
[3]J. Fuchs, "Ionospheric electron temperatures and the Hals-Stomer echo," National Research Council Pub. 581, **105**, 11 (1938).
[4]W. H. Preece, "Earth currents," Nature (London) **49**, 554 (1894).
[5]H. Barkhausen, "Pfeiftone aus dere Erde," Phys. Z. **20**, 402 (1919).

[6]T. L. Eckersley, "Musical atmospherics," Nature **135**, 104–105 (1935).
[7]E. V. Appleton, "Geophysical influences on the transmission of wireless waves," Proc. Phys. Soc. **37**, 16D–22D (1925); D. R. Hartree, "Propagation of electromagnetic waves in a refracting medium in a magnetic field," Proc. Cambridge Philos. Soc. **27**, 143–162 (1931).
[8]R. L. Stenzel, "Whistler wave propagation in a large magnetoplasma," Phys. Fluids **19**, 857–864 (1976).
[9]R. L. Stenzel, "Filamentation instability of a large amplitude whistler wave," Phys. Fluids **19**, 865–871 (1976); H. Sugai, K. Ido, H. Niki, S. Takeda, and K. Mima, "Dispersion and attenuation of whistler waves in a finite plasma," J. Phys. Soc. Jpn. **44**, 1953–1959 (1978).
[10]The LAPTAG website is at <coke.physics.ucla.edu/laptag>.
[11]M. Lieberman and A. Lichtenberg, *Principles of Plasma Discharges and Material Processing* (Wiley, New York, 1994), Chap. 12.
[12]J. A. Bittencourt, *Fundamentals of Plasma Physics*, 3rd ed. (FAPESP, Brazil, 1995).
[13]R. Fisher and R. Gould, "Resonance cones in the field pattern of a short antenna in an anisotropic plasma," Phys. Rev. Lett. **22**, 1093–1095 (1969).
[14]J. Wise, R. Hwang, M. Praglin, A. Lodge, R. Binaz, J. Novak, R. Baker, and W. Gekelman, "Measurement of plasma parameters in the LAPTAG plasma device," AAPT Southern California Section Meeting, May 2, 2009, contributed talk; J. Wise, A. Lee, G. Rosales, R. Wong, R. Baker, and W. Gekelman, "Measurement of edge plasma rotation," AAPT Southern California Section Meeting, May 2, 2009, contributed talk.
[15]R. Hwang, C. Eghtebas, A. Lee, W. Gekelman, P. Pribyl, J. Shin, J. Wise, R. Baker, and A. Martinez, "Experimental measurement and comparison to theory of whistler waves at the LAPTAG high school plasma laboratory," Bull. Amer. Phys. Soc. **55**(15), 169 (2010); A. Lee, W. Gekelman, P. Pribyl, C. Eghtebas, R. Hwang, J. Wise, R. Baker, and A. Strelsov, "Experiments on the ducting of Whistler waves at the LAPTAG high school plasma laboratory," *ibid*. **55**(15), 169 (2010); J. Wise, W. Gekelman, and R. Baker, "Using a plasma physics experiment to expand student understanding of the index of refraction," *ibid*. **55**(1), 66 (2010); C. Eghtbas, R. Hwang, J. Shin, W. Gekelman, P. Pribyl, J. Wise, R. Baker, and A. Lee, "Experimental measurement of Whistler waves at the LAPTAG high school plasma laboratory," *ibid*. **55**(1), 65 (2010); A. Lee, Y. Wang, C. Eghtbas, W. Gekelman, P. Pribyl, J. Wise, and R. Baker, "Comparison of measured Whistler wave energy flow to theory in the LAPTAG plasma device," *ibid*. **55**(1), 66 (2010).
[16]*Developing Talent in Young People*, edited by B. S. Bloom (Ballantine Books, New York, 1985).
[17]L. Brody, "Measuring the effectiveness of STEM talent initiatives for middle and high school students," Paper presented at 2006 September meeting of the National Academies Center for Education; <www7.nationalacademies.org/cfe/Linda%20Brody%20Think%20Piece.pdf>.
[18]A. Lee, R. Hwang, A. Cambonchi, R. Binaz, M. Praglin, J. Wise, and W. Gekelman, "The LAPTAG plasma physics laboratory," talk at the Southern California Physics Teachers Meeting, Occidental College (2009); W. Layton, W. Gekelman, J. Wise, N. Rodriguez, S. Cooperman, R. Griffen, J. Altonji, F. Carrington, B. Coutts, and K. Barker, "Encouraging high school students to consider physics related careers," Bull. Amer. Phys. Soc. **46**(8), 147 (2001); R. Baker, J. Altounji, R. Buck, C. Spahn, W. Gekelman, and P. Pribyl, "Construction of a high school plasma laboratory," *ibid*. **46**(8), 147 (2001); R. Baker, J. Wise, M. Buck, R. Buck, and W. Gekelman, "Characteristics of the LAPTAG high school plasma," *ibid*. **46**(8), 147 (2001); R. Buck, J. Wise, N. Gibson, M. Buck, W. Gekelman, E. Wetzel, C. Wetzel, and C. Moynihan, "Ion acoustic waves, A high school plasma experiment," *ibid*. **46**(8), 147 (2001); J. Wise, M. Buck, W. Gekelman, R. Buck, C. Spahn, C. Walker, and W. Layton, "Using plasma physics to enhance the high school physics curriculum," *ibid*. **46**(8), 147 (2001).
[19]B. Hannover and U. Kessels, "Self-to-prototype matching as a strategy for making academic choices. Why high school students do not like math and science," Learn. Instr. **14**, 51–67 (2004).
[20]Y. Ben-David Kolikant and S. Pollack, "Establishing computer science professional norms among high school students," Comput. Sci. Educ. **14**(1), 21–35 (2004).
[21]Movie of the vector magnetic field (drawn as white arrows) of a whistler wave launched from the loop antenna (described in the text) on the right side of the data plane. The movie frames are 0.4 ns apart. The data plane is the same as that in Fig. 10. The size of the data plane is $(\Delta x, \Delta z) = (17.2\ \text{cm}, 60\ \text{cm})$.